Article tracking [CONHYD_3049] - Expected dispatch of proofs

2 missatges

A.Nambiar@elsevier.com <A.Nambiar@elsevier.com> 15 de setembre de 2014 a les 20:45

Per a: jmcarmona@ub.edu, jmcarmonabcn@gmail.com

Article title: PROCESSES CONTROLLING THE FATE OF CHLOROETHENES EMANATING FROM DNAPL AGED SOURCES IN RIVER–AQUIFER CONTEXTS
Reference: CONHYD3049
Journal title: Journal of Contaminant Hydrology
Corresponding author: Dr. José M. Carmona
First author: Dr. Diana Puigserver
Received at Editorial Office: 16-FEB-2014
Article revised: 4-SEP-2014
Article accepted for publication: 9-SEP-2014
Expected dispatch of proofs: 22-SEP-2014

Dear Dr. Carmona,

The proof of your article will be sent to you for checking soon. This will be your last opportunity for incorporating minor corrections before final publication of your article. We expect the proof to be sent to you on 22-SEP-2014.
Please note that this date is subject to change due to variations in the production process. We will e-mail you with more information about your proof as it becomes available.

To track the status of your article throughout the publication process, please use our article tracking service:

http://authors.elsevier.com/TrackPaper.html?trk_article=CONHYD3049&trk_surname=Carmona

For more information on proofs: http://help.elsevier.com/app/answers/detail/a_id/140

Yours sincerely,
Ms Aparna Nambiar
E-mail: A.Nambiar@elsevier.com

PROCESSES CONTROLLING THE FATE OF CHLOROETHENES EMANATING FROM DNAPL AGED SOURCES IN RIVER–AQUIFER CONTEXTS

Diana Puigserver[a], Amparo Cortés[b], Manuel Viladevall[c], Xènia Nogueras[d], Beth L. Parker[e] and José M. Carmona[f]

[a] Dept. de Gequímica, Petrologia i Prospecció Geològica. Facultat de Geologia. Universitat de Barcelona. C/ Martí i Franquès, s/n. E-08028 Barcelona (Spain). e-mail address: puigserverdiana@ub.edu

[b] Dept. de Productes Naturals, Biologia Vegetal i Edafologia. Facultat de Farmàcia. Universitat de Barcelona. Av. Joan XXIII, s/n. E-08028 Barcelona (Spain). e-mail address: acortes@ub.edu

[c] Dept. de Gequímica, Petrologia i Prospecció Geològica. Facultat de Geologia. Universitat de Barcelona. C/ Martí i Franquès, s/n. E-08028 Barcelona (Spain). e-mail address: mviladevall@ub.edu

[d] Dept. de Gequímica, Petrologia i Prospecció Geològica. Facultat de Geologia. Universitat de Barcelona. C/ Martí i Franquès, s/n. E-08028 Barcelona (Spain). e-mail address: xenianogueras@ub.edu

[e] School of Engineering. University of Guelph. NIG 2W1 Guelph, ON (Canada). e-mail address: bparker@uoguelph.ca

[f] Corresponding author. Dept. de Gequímica, Petrologia i Prospecció Geològica. Facultat de Geologia. Universitat de Barcelona. C/ Martí i Franquès, s/n. E-08028 Barcelona (Spain). e-mail address: jmcarmona@ub.edu. Tel.: +34 93 4021399

Abstract

This work dealt with the physical and biogeochemical processes that favored the natural attenuation of chloroethene plumes of aged sources located close to influent rivers in the presence of co-contaminants, such as nitrate and sulfate. Two working hypotheses were proposed: i) Reductive dechlorination is increased in areas where the river–aquifer relationship results in the groundwater dilution of electron acceptors, the reduction potential of which exceeds that of specific chloroethenes; ii) zones where silts

predominate or where textural changes occur are zones in which biodegradation preferentially takes place. A field site on a Quaternary alluvial aquifer at Torelló, Catalonia (Spain) was selected to validate these hypotheses. This aquifer is adjacent to an influent river, and its redox conditions favor reductive dechlorination. The main findings showed that the low concentrations of nitrate and sulfate due to dilution caused by the input of surface water diminish the competition for electrons between microorganisms that reduce co-contaminants and chloroethenes. Under these conditions, the most bioavailable electron acceptors were PCE and metabolites, which meant that their biodegradation was favored. This led to the possibility of devising remediation strategies based on bioenhancing natural attenuation. The artificial recharge with water that is low in nitrates and sulfates may favor dechlorinating microorganisms if the redox conditions in the mixing water are sufficiently maintained as reducing and if there are nutrients, electron donors and carbon sources necessary for these microorganisms.

Key words: Reductive dechlorination; denitrification; sulfate reduction; immobile residual DNAPL; PCE isotopic enrichment; ecotone.

1. INTRODUCTION

Chloroethenes, such as perchloroethylene (PCE), are common groundwater contaminants due to their wide use in many industrial and commercial operations such as metal degreasing (e.g., trichloroethene or TCE) and dry cleaning (e.g., PCE). They often entered the ground in the solvent phase a few or more decades ago and are known as dense non-aqueous phase liquids (DNAPLs) due to their limited solubility and high density compared to water. They are carcinogenic compounds that linger in the environment once released and present a major threat to groundwater quality because of their high toxicity at very low concentrations, such that their health-based

water quality standards and analytical detection limits are several orders of magnitude below their respective aqueous solubilities (Pankow and Cherry, 1996). Their high density and low viscosity facilitate their downward migration through the subsurface (Mercer and Cohen, 1990; Pankow and Cherry, 1996; Luciano et al., 2010; Parker et al., 2003). In granular aquifers part of the DNAPL is retained at the pore-scale by capillary forces, which accounts for the existence of residual trails along the DNAPL migration pathways (Pankow and Cherry, 1996; Parker et al., 2003). As DNAPL descends, it may encounter layers of lower hydraulic conductivity that act as a barrier where DNAPL pools accumulate. Moreover, if the spill results in a large accumulation of DNAPL, lateral migration of pools takes place along the low-permeability layer until the DNAPL reaches a permeable window allowing deeper penetration in the system. Lateral migration always takes place along the path of least resistance, i.e., along the dip direction of these lower permeability layers. Lateral DNAPL migration distances of more than 100 m from input locations have been reported by Cohen and Mercer (1993) and by Jancin and Ebaugh (2002). The resultant DNAPL distribution or “architecture” of the DNAPL source zone is controlled by subtle geological heterogeneity that is accentuated by decades of DNAPL dissolution due to groundwater flow (Parker et al. 2003 and Guilbeault et al. 2005). An experimental field study of DNAPL source zone evolution using ground penetrating radar (Hwang et al. 2008) and later evaluated using a partitioning inter-well tracer test reported by Hartog et al. (2010) demonstrated that the remaining DNAPL saturations can be very low and sparsely distributed at aged sites after substantial dissolution with groundwater flow.

Chloroethenes are compounds that are recalcitrant over long periods (several decades or longer). Nevertheless, they can be biodegraded, which contributes to their natural attenuation. PCE and TCE are quickly broken down under anaerobic conditions when microorganisms that respire chloroethenes through biotic reductive dechlorination (Bradley, 2003 and 2011) have access to nutrients, electron donors, carbon sources

and growth factors (natural substances that stimulate the growth, proliferation, differentiation and cellular healing). Biotic reductive dechlorination is the most important process for the natural biodegradation of the more highly chlorinated chloroethenes (Wiedemeier et al., 1996). During this process, chloroethenes are used as electron acceptors, not as a carbon source, and one chlorine atom is replaced by one hydrogen atom. Reductive dechlorination takes place by sequential dechlorination from PCE to TCE, to dichloroethylene (DCE), to cis- DCE (cDCE) (a more common metabolite in biodegradation), to vinyl chloride (VC) and to ethene (or ethane, Vogel et al., 1987; Tiehm and Schmidt, 2011).

Depending upon the environmental conditions, this sequence may be totally or partially inhibited by competition for electron donors between dechlorinating and other indigenous microorganisms. This is one of the factors that determine the efficiency of in situ reductive dechlorination (Kouznetsova et al., 2010; Löffler et al., 1999). This competition takes place between communities of dechlorinating microorganisms and communities of anaerobic hydrogenotrophic (including reducers of NO_3^-, Mn^{4+}, Fe^{3+}, SO_4^-), autotrophic methanogenic and homoacetogenic microorganisms (Aulenta et al., 2006; Wei and Finneran, 2011).

PCE is the most oxidized chloroethene and more prone to reductive dechlorination. For the same reason, the decrease in the dechlorination rate is attributed to a lower oxidation (i.e., as the number of chlorine atoms is diminished) (Vogel and McCarty, 1985; Bouwer, 1994). As a result of this decrease in the biodegradation rate, cDCE and VC accumulate in the PCE plumes. This is usually attributed to partial reductive dechlorination (Bradley, 2011; Maymó-Gatell et al., 2001) and to the absence of strongly reducing conditions. Reductive dechlorination of chloroethenes takes place under nitrate (van der Zaan et al., 2010), manganese and iron reducing conditions (Bradley and Chapelle, 2011), although the fastest rates occur under sulfate-reducing and methanogenic conditions (Bouwer, 1994; Chapelle, 1996; Bradley, 2003).

As stated above, the microbial activity depends on the access to electron donors, i.e., on the availability of electrons for energy (Scheutz et al., 2010). The predominant electron donor in reductive dechlorination is molecular H_2 (Holliger and Schumacher 1994). In the natural attenuation, the formation of hydrogen is attributed to the subsurface fermenting community that uses natural organic matter (OM) to obtain energy (McCarty and Smith, 1986) and that controls the reducing activity in aquifers.

Moreover, the development of microbial communities is also conditioned by subsoil heterogeneities. Thus, DGGE analysis of porewater contaminated by chlorinated solvents carried out by Puigserver et al. (2013) showed that high microbial diversity and the development of communities take place in zones in which textural contrasts occur. These zones usually become ecotones (Goldscheider et al., 2006) where, among other biogeochemical processes, reductive dechlorination is favored.

The determination of the isotopic fractionation of parent and metabolite compounds is among the data used to identify bacterial biodegradation. Multi-isotopic analysis of ^{15}N, ^{34}S, ^{18}O, ^{13}C has proved to be a powerful tool for characterizing the processes of the biodegradation of nitrate, sulfate and chloroethenes (USEPA, 2008). In general, biodegradation is accompanied by a preferential degradation of molecules containing light isotopes (e.g., ^{12}C in the case of chlorinated solvents). The result is a progressive enrichment in the heavier isotopes through time or a flow line in the aquifer (USEPA, 2008). Multi-isotopic techniques allow us to determine the isotopic signature of an element, e.g., carbon, by measuring the two stable isotopes, ^{12}C and ^{13}C. This relationship is expressed as $\delta^{13}C$ (in ‰ units) = $(R_{sample} / R_{standard} - 1) \times 1000$, where R_{sample} is the $^{13}C/^{12}C$ ratio in a given sample and $R_{standard}$ is the $^{13}C/^{12}C$ ratio in the international standard V-PDB (USEPA, 2008). Higher values of $\delta^{13}C$ (less negative) indicate increases in an isotope with respect to the standard, whereas lower values (more negative) indicate decreases and a less advanced biodegradation process. Isotopic enrichment varies depending on the compound, the enzymatic biodegradation

pathway (Chartrand et al., 2005), the geochemical parameters (such as redox conditions), the development of microbial populations or on the abiotic reactions. This progressive enrichment is expressed by the Rayleigh equation (Mariotti et al., 1981; Steinbach et al., 2004).

Plumes emanating from DNAPL pollution sources of chlorinated solvents can affect groundwater and surface water. In many cases these sources are located in zones adjacent to rivers, where a close interaction between groundwater and surface water exists. Groundwater management requires an adequate understanding of the interactions between rivers and aquifers, particularly in the groundwater-surface water interface (GW-SW) (Smith et al., 2009). This interface encompasses the river bed, the hyporheic zone and the river banks, although it may extend into the riparian zone, depending on the structure of the materials of the subsurface, hydraulic conductivity and hydraulic gradient between river and aquifer. This interface is a dynamic transition zone that controls the migration and the fate of contaminants (Fleckenstein et al., 2006).

The first studies linking the hydrological dynamics at the GW-SW interface with biogeochemical processes were undertaken in the1980s. Most of this research was devoted to the study of the chemistry of nitrogen in the near stream zone (Hill, 1990) and the exchanges occurring between the streambed and sediment (Bencala, 1984). The exchange processes that occur at a small scale at the GW-SW interface and associated biogeochemical processes began to be studied in the 1990s. These works were focused on the hyporheic zone and on the streambed. Subsequently, further research was carried out on GW-SW interactions in disciplines such as hydrology, hydrogeology, ecology and biogeochemistry. Research has also incorporated geological heterogeneities at different scales into models of GW-SW interactions (Fleckenstein et al., 2006; Engdahl et al, 2010). However, this research is still in its infancy. Furthermore, models based on processes linking hydrologic dynamics and

biogeochemical processes are still incipient (Cardenas et al, 2008; Boano et al., 2010) and are not yet fully applicable to complex situations in the field.

Most of the aforementioned research refers to effluent rivers and to processes in the hyporheic zone. Moreover, most of the studies undertaken on influent rivers concern aquifer contamination by pollutants discharged into the river (e.g., industrial spills). In addition, many of these studies are in situations where induced recharge for the water supply was promoted with the result that they are focused on the analysis of clogging in producing wells and on pollution from the river (Stuyfzand et al., 2006).

A number of pollutants are attenuated at the GW–SW interface because of degradation and retardation. These pollutants include nitrate and metals from mining. Furthermore, despite the relatively common occurrence of sites contaminated by chlorinated solvents, few published studies have described in detail the hydrological and geological controls on plume characteristics at the GW-SW interface (Fleckenstein et al., 2006). Of these studies, very few dealt with plumes of chlorinated ethenes discharging into rivers, although these studies discussed advection, biodegradation and sorption affecting these compounds.

In summary, no earlier studies were published that included a source of PCE DNAPL located on the banks of an influent river. Neither have studies been published that describe the interaction between chloroethenes and co-contaminants (such as nitrates and sulfates), which can adversely affect the natural attenuation of chloroethenes.

The present work seeks to fill this gap by offering fresh insights into the distribution of chloroethene plumes in aged sources located close to influent rivers, with the aim of improving future remediation strategies. We address the manner in which subsoil heterogeneities and physical, biogeochemical and hydrogeological conditions affect the main processes that influence the spatial and temporal evolution of chloroethenes and other co-contaminants. Two working hypotheses were proposed: i) Reductive dechlorination is increased in areas in which the river–aquifer relationship results in the

groundwater dilution of electron acceptors that have reduction potentials that exceed those of specific chloroethenes; ii) zones in which silts predominate or in which textural changes take place are zones in which biodegradation preferentially occurs.

A field site on a Quaternary alluvial aquifer was selected at Torelló, Catalonia (Spain), approximately 80 km to the north of Barcelona. This is a zone in which PCE DNAPL was detected in an immobile residual form. This zone is adjacent to a river in an area where it is influent to groundwater and where the redox conditions favor reductive dechlorination.

2. SITE DESCRIPTION

Groundwater PCE contamination at the site was attributed to chlorinated organic solvents used as degreasers at a nearby industrial plant. The contamination, which was detected in a municipal water supply well in 2000, was attributed to three source areas containing PCE free phase and immobile residual DNAPL (Puigserver et al., 2008), i.e., source areas A, B and C (Figure 1). These areas comprise an irregular Quaternary alluvial overburden that constitutes an unconfined aquifer connected to the River Ges and to fractured marls and marlstones of the Eocene, which make up the bedrock. The overburden consists of fine sands and silts crossed by interconnected paleochannels (Figure 1) containing sands and gravels with interbedded thin clayey-silty layers. Fractured marls and marlstones contain disseminated microscopic pyrite and the fracture network consists of two orthogonal subvertical diaclase systems (160º NW-SE and 216º NE-SW). The average fracture spacing is 1 m, and the mean aperture is approximately 1 or 2 cm at the surface (Puigserver et al., 2008).

Figure 1.

The plant has been in operation since 1967 and dirty PCE releases through the old dug well T41 in source area B (Figure 1) may have continued into the 1980s or later. These

releases were not sporadic but were fairly regular over time. The large amount discharged over decades led to the accumulation of free phase DNAPL on the silt layers interbedded in the gravels of the paleochannels and on the marlstones. The slight dip of all of these materials towards source area C (the study zone, Figure 1A) caused a lateral migration of free phase DNAPL from well T41 in source area B to source area C through paleochannels connecting both banks of the River Ges (Figure 1). Pools of mobile free phase DNAPL reached source area C several decades ago, although today they are aged sources constituted by the immobile residual phase.

3. MATERIALS AND METHODS

3.1 Monitoring networks

Our study made use of two monitoring networks. One of these networks was installed by the Catalan Water Agency (ACA) and consists of former dug wells and conventional piezometers (SD code in Figure 1) of PVC tubes, 110 mm in diameter. Screened zones range between 2 m and 10 m from the bottom of the piezometer, which allowed us to obtain combined samples from both aquifers. The depth of these piezometers varied between 3 m and 52 m. Our research group installed a supplementary network of conventional piezometers (S code in Figure 1) to sample only the alluvial aquifer. This network consisted of completely screened polyethylene tubes, 75 mm in diameter, with depths ranging between 2.6 m and 4.5 m. Selected piezometers of the monitoring networks were distributed in profiles (profiles A-A', B-B' and C-C', Figure 1). The monitoring networks were sampled every two months between 2005 and 2007 and in the fall of 2008 and 2009.

3.2 Field measurements and samples

To set the two hypotheses in the context of the biogeochemical processes influencing the fate of chloroethenes, we conducted an analysis of the river-aquifer relationship characterizing the study zone. We obtained geological, stratigraphic and geophysical data, as well as river and groundwater temperature, electrical conductivity (EC) and aquifer water table levels. As a result, the conceptual model of the river-aquifer relationship was devised. The river and groundwater dissolved oxygen (DO) and redox potential (Eh) were also determined to study the redox conditions. Moreover, to ascertain whether redox conditions reached the Mn and Fe stages in the source zone, groundwater and soil samples were analyzed for Mn and Fe for comparison with the background values. Soil samples were also used to determine the fraction of organic carbon (f_{oc}). To investigate the biogeochemical processes that condition the fate of chloroethenes, groundwater samples were taken to analyze dissolved total organic carbon (TOC), nitrate, $\delta^{15}N_{NITRATE}$, $\delta^{18}O_{NITRATE}$, sulfate, $\delta^{34}S_{SULFATE}$ and $\delta^{18}O_{SULFATE}$. In addition, river water was sampled to analyze TOC.

The first working hypothesis was tested by studying the fate of chloroethenes in the source zone (profile A-A' along the riverbank in Figure 1B) and along flow (profiles B-B' and C-C' in Figure 1B), focusing on the spatial and temporal variability of the hydrochemical and isotopic characteristics of DNAPL and co-contaminants. This variability and the manner in which it was conditioned by the recharge from the River Ges were analyzed using groundwater samples to determine PCE, $\delta^{13}C_{PCE}$, and the aforementioned nitrate, $\delta^{15}N_{NITRATE}$, $\delta^{18}O_{NITRATE}$, sulfate, $\delta^{34}S_{SULFATE}$ and $\delta^{18}O_{SULFATE}$. Furthermore, Sudan IV was employed to detect the presence of immobile residual DNAPL phase in core samples from boreholes. Samples of immobile residual DNAPL from borehole S2 (in which residual DNAPL was detected, Figure 1B) were used to analyze the DNAPL chloroethene molar fractions and $\delta^{13}C$ value of the spilled DNAPL.

To test the second hypothesis, a comparative analysis of reductive dechlorination in the zones in which gravels predominated and in the zones in which fine sands and silts prevailed was conducted for one year. To conduct this analysis, in addition to the aforementioned parameters and compounds, groundwater samples were collected to analyze the chloroethene metabolites of PCE (i.e., TCE, cDCE and other isomers, and VC) and the values of $\delta^{13}C_{TCE}$ and $\delta^{13}C_{cDCE}$ ($\delta^{13}C_{VC}$ could not be determined because of the low concentrations of this compound).

3.3 Protocols and procedures

3.3.1 Sampling protocols

Samples to determine the Mn and Fe adsorbed on the fine mineral fraction in the saturated zone and f_{oc} were obtained manually using an Eijkelkamp hand auger at depths between 1 m and 1.7 m and during the drilling of our piezometer network. The sampling protocols were described in Mason (1992). The sampling procedure of residual DNAPL and the conservation protocol, as well as the calculations of porewater (and sorbed) concentrations of chloroethenes, were adapted from the protocol of Parker et al. (2003) and Chapman and Parker (2005) for granular contexts. To minimize volatilizations, we used a methanol trap (MeOH, Merck, ISO Pro analysis) in accordance with EPA SW-846, Method 5035.

Groundwater samples were taken using an Eijkelkamp peristaltic pump and an Integra Solinst Bladder pump, depending on the depth of the piezometers. Aqueous samples were collected in 100 mL VOCs glass serum bottles (SUPELCO analytical) for concentration analysis and in 120 mL amber screw cap bottles (SUPELCO analytical) for carbon isotope and TOC analysis. We used Pyrex glass bottles for $\delta^{15}N_{NITRATE}$, $\delta^{18}O_{NITRATE}$ and $\delta^{34}S_{SULFATE}$ and $\delta^{18}O_{SULFATE}$ analysis. Groundwater samples for nitrate and sulfate analysis were collected in 150 mL translucent plastic bottles. Mn and Fe samples were collected in 14 mL transparent plastic vials. Samples were conserved at

4ºC. We followed the sampling and conservation protocols indicated in Puls and Barcelona (1996) and Johnston (2006).

3.3.2 Analytical methods in laboratory for chemical and isotope analyses. Techniques and instrumentation

Samples were analyzed at the laboratories of the Scientific-Technical Services of the University of Barcelona. Core samples, to determine Mn and Fe, were attacked with *aqua regia* to extract the adsorbed Fe and Mn in accordance with the ISO/DIS 11466 protocol. Mn and Fe in soil samples and in groundwater samples were analyzed using Inductively Coupled Plasma Mass Spectrometry (ICP-MS).

Pretreatment of core samples to determine f_{oc} consisted of removing the inorganic carbon fraction by adding HCl (37%, Sigma-Aldrich) according to the ISO 10694:1995 protocol. The resulting fraction was analyzed by Gas Chromatography (GC) with a Thermal Conductivity Detector (TCD). TOC was analyzed using the TOC analyzer TOC-5000 (Shimadzu). The extraction of chloroethenes in the core samples (sorbed and in porewater) was carried out in the laboratory by adapting the protocol described in Dincutoiu et al. (2003). Gas chromatography–mass spectrometry (GC-MS) was used to identify the chloroethenes.

Nitrate, nitrite and sulfate were analyzed by ion chromatography. Ammonium was determined by flow spectrophotometry. The determination of $\delta^{13}C$ in chloroethenes was carried out by Gas Chromatography Combustion Isotope Ratio Mass Spectrometry (GC-C-IRMS) in accordance with the protocol described in Palau et al. (2007). The pretreatment protocols used to determine the nitrate and sulfate isotopic compositions were those indicated in Dogramaci et al. (2001) for determining $\delta^{34}S_{SULFATE}$ and $\delta^{18}O_{SULFATE}$ and in Silva et al. (2000) and Fukada et al. (2003) for obtaining $\delta^{15}N_{NITRATE}$ and $\delta^{18}O_{NITRATE}$ precipitates. These samples were analyzed by Isotope Ratio Mass Spectrometry (IRMS).

4. RESULTS

4.1 Results to frame the hypotheses in the context of the river-aquifer relationship

4.1.1 Geological data to characterize the aquifer formation

The Quaternary alluvial formation was distributed over two terraces that are geomorphologically differentiated. Stratigraphic and textural description of cores from boreholes and hydraulic conductivity from slug tests, together with the interpretation of electrical tomography resistivity surveys, showed that the alluvial materials of the Quaternary were made up of paleochannels of gravels and sandy gravels containing some interbedded thin clayey-silty layers. These paleochannels were situated at different depths between fine sands and silts and silty-sandy materials. The bedrock was formed by fractured marls and marlstones containing disseminated microscopic pyrite. The river bed was composed of materials of the alluvial formation in the stretch between source areas B and C, whereas the river flows directly over the marls and marlstones of the bedrock along the rest of the fluvial course. Consequently, the two banks of the river were connected by the paleochannels (Figure 1).

4.1.2 Hydrodynamic and hydrochemical data to analyze the river-aquifer relationship and to characterize the aquifer formation

The groundwater flow was mainly horizontal or subhorizontal in the alluvial aquifer. However, upward flow components existed on the east bank in source area B, as shown by water table levels at piezometers SD2 and SD3 (screened in the fractured marlstones and in the alluvial aquifer, respectively), in which the water table at SD2 was always higher than the water table at SD3. This figure also shows the water table map in which the general flow of groundwater was mainly westward on the east bank of the River Ges, showing the effluent nature of the river on this bank. In contrast, groundwater flows westward in the west bank in the zone adjacent to the river, where it

always showed an influent nature, i.e., under low, medium and high water table conditions (LWT, MWT and HWT, respectively). Flow lines converged, adopting a southward direction upon reaching the main gravel paleochannels (which act as drainage lines) of the alluvial aquifer in this bank.

The minimum water table levels were recorded in summer and winter (from June to September and from December to March, respectively). In contrast, in spring and fall (from March to June and from September to December, respectively), the water table levels were higher (i.e., when rainfall is more abundant).

Figure 2 (profile C-C') shows that temperature and EC in the River Ges underwent considerable fluctuations over time. Furthermore, groundwater temperature varied widely in the source zone (Figure 2, profile A-A' along the riverbank), but this variability decreased with increasing distance from the river, when the temperature was homogenized along the flow by hydrodynamic dispersion (Figure 2, profile C-C'). This figure also shows that groundwater EC displayed a constant variability along the profile A-A' (with the exception of SD29). Furthermore, the increase in EC, nitrate and sulfate with increasing distance from the river (profile C-C' in Figure 2, Figure 4A and Figure 5A, respectively) together with the diminishing variability of temperature in the aquifer is consistent with the fact that the river is always influent.

Figure 2.

The effective porosity, calculated from granulometric analysis (Robson, 1993), oscillated between 0.14 and 0.28. The hydraulic conductivity of the alluvial aquifer, determined by slug tests, fluctuated between 5 m/day and 490 m/day (average values of 10 m/day and 100 m/day for silty materials and gravels, respectively). Average Darcy velocities in the source zone were calculated from hydraulic conductivities and

hydraulic gradients, graphically determined from a detailed water table map of source area C. The velocities ranged from 0.27 m/day to 1.6 m/day for zones of silty materials and for gravel paleochannels, respectively. The retardation factor for PCE ranged from 1.1 to 1.62 for gravels and silts, respectively, and they were determined using the linear sorption isotherm. For this factor, the formula $R = 1+((\rho_a/\varphi)\cdot K)$ (Fetter, 1999) was used. In this formula, R is the retardation factor, ρ_a is the bulk density of the sediment (g/mL), φ is the porosity of the sediment and K_d is the partition coefficient between PCE dissolved and PCE sorbed in the sediment (mL/g) for the linear isotherm. The partition coefficient (K_d) was calculated using the formula $K_d = K_{oc}\cdot f_{oc}$ (Fetter, 1999), where f_{oc} is the organic carbon fraction in sediment and K_{oc} is the sediment organic carbon-water partitioning coefficient.

4.2 Results to analyze the redox conditions controlling the biogeochemical processes

4.2.1 TOC and DO data

The TOC concentrations in the River Ges were higher in summer, coinciding with minimum values of DO and high temperatures. Groundwater TOC concentrations (Figure 3) ranged from 5 mg/L to 15 mg/L (on average 10 mg/L).The highest values coincided with the periods when the fields were manured (September–October). The water values of TOC in the River Ges were lower than in the groundwater (Figure 3, profiles B-B' and C-C'). According to the TOC concentrations in groundwater, DO depletion to low values was recorded between 0.05 mg/L and 2.15 mg/L (Figure 3). This resulted in reducing conditions that prevailed throughout the year with Eh negative or close to 0 mV, especially in the summer (low water table period, LWT).

Figure 3.

4.2.2 Nitrate and sulfate data

As in the case of EC (Figure 2, profile C-C'), nitrate and sulfate increased with distance from the River Ges (Figure 4A and Figure 5A). The average nitrate value was 110 mg/L (1.8 mmol/L), but in late summer and early fall (September–October) concentrations were higher, which coincided with the manuring period, e.g., 450 mg/L (7.26 mmol/L) in SD29. Isotope fractionation of nitrogen and oxygen of nitrate also occurred, as shown in Figure 4B. Most of the samples were aligned fairly well along a straight denitrification line originating in the manure and septic waste field of the figure.

Figure 4.

The average sulfate value resembled that of the alluvial background, 81 mg/L (0.84 mmol/L), ACA (2005), and remained fairly constant throughout the year. As was the case for nitrate, isotope fractionation of sulfur and oxygen of sulfate also occurred. Figure 5B shows the groundwater samples arranged along a straight line depicting a sulfate-reducing trend, which originated in the sulfide oxidation field of the figure.

Figure 5.

4.2.3 Mn and Fe data

Soil surveys revealed lower average values for the Mn and Fe concentrations (15,943 and 246 mg/kg in Mn and Fe, respectively) in the source zone than those of the background upgradient of this zone (18,383 and 276 mg/kg, respectively).

The highest Mn content (988.8 µg/L) in the groundwater of the source zone coincided with high TOC concentrations and was recorded in a medium water table period (MWT) in September 2006 at piezometer SD29. The highest Fe content (1237 µg/L) in the groundwater of the source zone was recorded in a LWT period in July 2006 at SD28. During the high water table period (HWT) of May 2006, the average value of Mn in groundwater (147.9 µg/L) occurred and coincided with high TOC contents. The

average concentration of Fe during periods of HWT (May 2006) was 410.48 µg/L. These average groundwater concentrations were found to be higher than those of the background (20.6 µg/L and 25.3 µg/L for Mn and Fe, respectively).

4.3 Results to corroborate the two hypotheses

In the source zone (profile A-A' along the riverbank), the most abundant dissolved chloroethene was PCE. In fact, the immobile residual DNAPL was mainly composed of PCE followed by TCE, cDCE (average molar fractions in S2 core samples of 99%, 0.1% and 0.1%, respectively) and other VOCs. The highest molar fractions and concentrations of dissolved PCE were registered at SD29 (Figure 6A). The cDCE concentrations generally exceeded those of TCE (on average four times higher).

Figure 6.

4.3.1 Concentration and isotopic composition data of chloroethenes in paleochannels of gravels and sands

The PCE molar fraction was normally high and relatively constant over time at piezometers S3 and SD32, located in paleochannels of gravels and sandy gravels. Nevertheless, at SD29, which is also located in these paleochannels and at which residual DNAPL was recorded (Table 1), the PCE molar concentration increased and the PCE molar fraction varied little during the water level recovery period from July to September 2006 (Figure 6A). VC was detected at the piezometers that showed no residual DNAPL when drilled (SD32 and S3), which coincided with reducing conditions in September 2006 (Figure 6A) after a LWT period. These piezometers showed $\delta^{13}C_{PCE}$ values that were slightly heavier than those where residual DNAPL was detected (SD29) (Figure 6B). In these cases, $\delta^{13}C_{TCE}$ and $\delta^{13}C_{cDCE}$ values were lighter than the $\delta^{13}C_{PCE}$ values (Figure 6B).

4.3.2 Concentration and isotopic composition data of chloroethenes in zones of predominant fine sands and silts

The piezometers in the zones predominantly comprised of fine sands and silts (SD28, S1, SD30 and SD31) recorded higher molar fractions and concentrations of metabolites than piezometers in gravel paleochannels (SD29, S3 and SD32) (Figure 6A). The highest molar fractions and concentrations of chloroethene metabolites were recorded at these piezometers, especially during the LWT periods (e.g., SD31). However, increases in the total molar concentration coinciding with rises in the water table also took place, e.g., SD30 from July to September 2006 (Figure 6A). By contrast, a marked decrease in the concentration of chloroethenes occurred on other occasions during the recovery periods (e.g., SD31 in March 2006 and from July to September 2006). The PCE molar fraction and the formation of VC at piezometer SD31 were relatively constant over time (Figure 6A). The piezometers located in these materials showed a greater isotopic fractionation than those in the gravel paleochannels. Thus, the greatest PCE degradation took place in the source zone, adjacent to the River Ges, at SD31, where $\delta^{13}C_{PCE}$ reached -18 ‰ (Figure 6B) with a $\Delta\delta^{13}C_{PCE}$ of 6.29 ‰ with respect to the $\delta^{13}C_{PCE}$ value in the DNAPL.

4.3.3 Isotopic fractionation data of chloroethenes, nitrates and sulfates in the source zone

In the source zone, the isotope composition of PCE of the residual DNAPL was -25.66 ‰ (Figure 6B, average in S2 core samples). This value was close to that of the lightest isotope composition of dissolved PCE at piezometers at which residual DNAPL was found (SD28 with -24.25 ‰).

4.3.4 Isotopic fractionation data of chloroethenes, nitrates and sulfates along the flow

Piezometers along flow tended to show higher PCE molar fractions (Figure 7A and Figure 8A) than piezometers in the source zone (Figure 6A, profile A-A´ along the riverbank). Furthermore, only a slight isotope fractionation of PCE occurred between S4 and SD19 in profile B-B´ (Figure 7B).

Figure 7.

In this profile, the $\delta^{13}C_{TCE}$ and $\delta^{13}C_{cDCE}$ values exceed those of $\delta^{13}C_{PCE}$, and $\delta^{13}C_{cDCE}$ was higher than $\delta^{13}C_{TCE}$ (Figure 7B). Higher PCE molar concentrations and lighter $\delta^{13}C_{PCE}$ values were recorded downgradient of the source zone (between SD32 and S5, where residual DNAPL was detected, Figure 8A and 8B). Moreover, heavier $\delta^{13}C_{PCE}$ values and higher PCE molar concentrations were recorded between S5 and S6 (where residual DNAPL was not recorded).

Figure 8.

These progressively heavier $\delta^{13}C_{PCE}$ values along flow were accompanied by $\delta^{15}N_{nitrate}$ and $\delta^{34}S_{sulfate}$ values that also became heavier (Figure 9A). By contrast, in the source zone, the $\delta^{15}N_{nitrate}$ and $\delta^{34}S_{sulfate}$ values were generally low (Figure 9A) and accompanied by a wider variation in $\delta^{13}C_{PCE}$ (Figure 9B and 9C).

Figure 9.

5. DISCUSSION

5.1 Biogeochemical processes interacting with chloroethenes

5.1.1 Oxidation of organic matter

The high TOC concentrations in groundwater were due to sheep grazing and the application of animal manure to fields at regional and local scales. Depletion of DO occurred because of the oxidation of dissolved and solid OM, which gave rise to prevailing reducing conditions over the year and favored anaerobic biodegradation, especially in summer (from June to September, LWT period). At this time, temperature and actual evapotranspiration were the highest and precipitation was the lowest. Thus, the aquifer recharge through the unsaturated zone was minimal and the input of oxygen to the aquifer through this zone was minimal. The high temperature caused diminished solubility of oxygen in the river. The lower velocity in the river, in addition to discharges of liquid wastes, favored a greater consumption of DO by microorganisms. The mass of DO that reached the aquifer due to the recharge from the river was therefore small. This situation, together with the higher temperature of groundwater in summer, contributed to the biogeochemical processes leading to the oxidation of OM and the depletion of DO and to reduction reactions when conditions became strongly reducing. The oxic-anoxic boundary varied throughout the year because the TOC input and the water table level fluctuated over time (Figure 3).

Spatial patterns along flow were similar in TOC, nitrate and sulfate (Figure 3, Figure 4A and Figure 5A). However, while the low concentrations of nitrate and sulfate in the zone close to the River Ges were caused mainly by dilution, the low TOC concentrations were also due to the high consumption of organic carbon (as dissolved or solid OM) that took place in this zone.

5.1.2 Reducing processes affecting Mn, Fe and co-contaminants

Nitrate produced by the nitrification of ammonium due to manuring was superimposed onto a high regional nitrate background. As a result of the prevalent reducing conditions, the denitrification process occurred and $\delta^{15}N_{nitrate}$ progressively became heavier downgradient from the source zone (Figure 9A), similar to that described in Wexler et al. (2012). The low concentrations of nitrite found in the study zone demonstrated that this compound rapidly decreases according to Davidson et al. (2003), leading to the formation of N_2. Denitrification prevailed over reductive dechlorination (Bradley, 2011; Yang and McCarty, 1998). However, in the study zone, the input of water from the River Ges resulted in nitrate dilution in the source zone and in an increase in nitrate concentrations downgradient (Figure 4A). Dilution leads to less competition for electrons by nitrate (as the preferential acceptor in the respiratory chain of the denitrifying microorganisms) in zones close to the river, which favored the activity of other microorganisms.

The reduction of Mn and Fe also occurred in the study zone. However, because the oxic-anoxic boundary fluctuated throughout the year due to the variable inputs of TOC (see Section 5.1.1), these processes varied in space and time, mainly in the source zone, where the solid and dissolved OM predominated (e.g., at piezometers SD29 and SD28). Furthermore, in summer, when the water table level and DO were low, the reduction of Fe predominated. The reduction of Mn prevailed in spring when the water table level was high.

The occurrence of these processes was consistent with the high values found in groundwater and with the oxidation of solid and dissolved OM under anaerobic conditions (Lin et al., 2012).

Another biogeochemical process that took place was sulfate reduction, which accounted for the isotope fractionation trend of sulfur shown in Figure 5B. This trend originated in the sulfide oxidation field of the figure, which showed that sulfate results

mainly from the continuous input from the oxidation of pyrite (also observed in Canfield, 2001; Gibson et al., 2011). For this reason, despite sulfate reduction, sulfate concentrations remained fairly constant over time. However, a rise in sulfate concentration occurred along the flow despite the loss of sulfate due to sulfate reduction (Figure 5A). This apparently contradictory behavior was explained, as in the case of nitrate, by the dilution effect and by the continuous input of sulfates from groundwater circulating through marlstones.

Denitrification and sulfate-reducing processes were still incipient (i.e., light $\delta^{15}N$ $\delta^{34}S$ values) in the source zone, whereas downgradient, the higher isotopic fractionation provided ample evidence of an increase in denitrification and sulfate reduction along flow, as shown in Figure 9A.

5.2 Reductive dechlorination

5.2.1 Reductive dechlorination is favored by dilution in the source zone (first hypothesis)

In the source zone, the low concentrations of nitrate and sulfate, because of the dilution effect (Figure 4A and Figure 5A), diminished the competition for electrons between consortia of denitrifying and sulfate-reducing microorganisms and those of dechlorinating microorganisms. The most bioavailable electron acceptors under these conditions were PCE and metabolites. This meant that their biodegradation was favored (as shown in Figure 9B and 9C, profile A-A'), which corroborated our first working hypothesis. In contrast, both nitrate and sulfate competed with PCE with the increase in distance from the source. This is demonstrated by the heavier $\delta^{15}N_{nitrate}$ and $\delta^{34}S_{sulfate}$ values of the samples located downstream of the source for a given $\delta^{13}C_{PCE}$ value (Figure 9B and 9C, profiles B-B' and C-C'), which lent further support to our first hypothesis.

5.2.2 Reductive dechlorination is favored in the zones of predominant fine sands and silts (second hypothesis)

Regardless of whether the area was dominated by silts or gravel paleochannels, concentrations of TOC in groundwater in the source zone were similar (as shown in profile A-A' of Figure 3). However, if the solid OM in the zones in which silts dominated is compared with solid OM in the gravel paleochannels, the content in the former is higher than in the latter, which are 0.12 % and 0.02 %, respectively (expressed as the fraction of organic carbon). Consequently, the total amount of organic carbon available to the microorganisms in both areas (as a source of carbon and energy) was the sum of dissolved organic carbon and solid organic carbon (i.e., present in the solid OM). Therefore, this sum was always higher in areas in which silts were dominant.

Gravel paleochannels zones had higher flow velocities, and the sum of organic carbon was lower, making it difficult for dechlorinating microorganisms to gain access to the elements they need. The consequence was a decrease in dechlorination as shown by the low molar fraction of chloroethene metabolites and the usually high and fairly constant PCE molar fraction at SD29, S3 and SD32 over time (Figure 6A).

By contrast, in the zones in which fine sands and silts were dominant, hydraulic conductivity was lower, whereas dissolved TOC and solid OM available to microorganisms, as well as matrix retardation factor due to sorption, were often higher (Cherry and Parker, 2006; Parker et al., 2004). As a result, biodegradation was favored in these areas. In addition, the zones where textural changes exist constitute ecotones in which indigenous dechlorinating microorganisms have a more favorable substrate for their development (Flynn et al., 2000; Puigserver, 2010; Puigserver et al., 2013). In these ecotones, silts are rich in solid OM and the low flow restricts oxygenation of the medium. Furthermore, conditions to access nutrients and electron acceptors supplied by groundwater in fine sands are more stable over time. As a result, biogeochemical conditions are more favorable to reductive dechlorination. This was observed at SD28, S1, SD30 and SD31 (see Figure 6A), where the greater effectiveness of the reductive

dechlorination favors biodegradation of PCE to TCE and TCE to cDCE, resulting in a predominance of cDCE over TCE (Hunkeler et al., 2005; Bradley, 2011). This, plus the heavier $\delta^{13}C_{PCE}$ values at SD31 (Figure 6B) where biodegradation was greater, also corroborated the more favorable conditions for reductive dechlorination in silty zones. These results validated our second hypothesis.

5.2.3 Variability of reductive dechlorination throughout the year

The most favorable reducing conditions for the formation of chloroethene metabolites occurred during the summer months (from June to September), in which stronger reducing conditions were dominant in the source area (see section 5.1.1). This is the case of piezometers in the source zone (Figure 6A profile A-A' adjacent to the river) during the LWT and MWT periods of July and September 2006 and October 2008. During this period, the total molar concentrations and the molar fractions of metabolites tended to be higher than in the recovery periods of March and May 2006. In addition, the low values of the water table levels led to an increase in the concentration of chloroethenes, especially in the source zone. Thus, dissolution of PCE-DNAPL continued as groundwater flowed through the source during the periods when the water table was low. Because the volume of groundwater in the source zone decreased at that time, PCE and metabolite concentrations increased.

Sulfate-reducing conditions were dominant, and competition for electrons diminished because of the dilution effect in the source zone (see section 5.2.1) during these periods. This accounted for the increase of PCE metabolites compared to other periods. Moreover, the stage in which VC is formed was attained in the sequential reductive dechlorination of PCE (in agreement with Bouwer, 1994; Chapelle, 1996; Bradley, 2003; Bradley and Chapelle, 2011). For example, VC was formed specifically in the piezometers of profile A-A´ during the LWT and MWT periods of July and

September 2006 and October 2008 (Figure 6A). This would allow the complete reductive dechlorination sequence to occur (Pantazidou et al., 2012).

By contrast, a decrease in the concentration of chloroethenes due to dilution, together with a certain oxygenation of the medium that occurred during the recovery periods, generally resulted in a low rate of metabolite formation, e.g., in March and May 2006, corresponding to HWT and MWT periods, respectively (Figure 6A).

However, increases in the molar fraction of metabolites were also recorded in other cases during the recovery periods. An example of this is SD28 in September 2006. Residual phase was detected at this piezometer when drilling the borehole (Table 1), which strongly suggested that the increased concentrations of metabolites were attributed to a greater bioavailability of PCE (Fowler and Reinauer, 2013) because of the proximity to the source.

6. CONCLUSIONS

Groundwater dilution by surface water gave rise to the lower bioavailability of nitrate and sulfate. Moreover, because reducing conditions dominated, the prevailing biogeochemical process was reductive dechlorination. This illustrated the significance of the aquifer–river interaction in the natural attenuation of chloroethenes in the presence of other electron acceptors whose reduction potential exceeds that of chloroethenes. A strategy is therefore proposed to bioenhance natural attenuation at sites in granular media that have sources of chloroethenes that are not necessarily adjacent to the surface (or marine) waters and where the hydrochemical context is rich in other electron acceptors that compete with chloroethenes. Thus, the artificial recharge with water low in nitrates and sulfates immediately upgradient from the DNAPL-source may favor indigenous dechlorinating microorganisms if the redox conditions in the mixing water are maintained as sufficiently reducing and if nutrients, electron donors and carbon sources necessary for these microorganisms are provided.

Zones with textural changes in silty materials were areas of preferential biodegradation in which indigenous microorganisms that biodegrade chloroethenes developed because of a more favorable substrate.

ACKNOWLEDGEMENTS

We are indebted to ACA, the Tubkal Consultant Company, the Torelló municipality and to all persons who facilitated measuring and sampling in the wells.

We wish to acknowledge the laboratories of the University of Barcelona (Serveis Científico-Tècnics) for assistance with sample analysis.

The results presented in this article are part of the project "Integration of characterization techniques in DNAPL episodes of soil and groundwater contamination for the definition of aquifer remediation proposals" funded by the Spanish Ministry of Education and Science (CTM 2005-07824 and CGL2008-02164/BTE).

REFERENCES

ACA. Catalan Water Agency. 2005. Bodies of groundwater of Catalonia. Characterization, Analysis of pressures, impacts and analysis of the risk of non-compliance. Plana de Vic-Collsacabra. Departament de Medi Ambient i Habitatge (Generalitat de Catalunya). Barcelona (Spain).

Aulenta, A., Majone, M., Tandoi, V., 2006. Enhanced anaerobic bioremediation of chlorinated solvents: environmental factors influencing microbial activity and their relevance under field conditions. J. Chem. Technol. Biotechnol. 81, 1463–1474.

Bencala, K.E., 1984. Interactions of solutes and streambed sediment. 2. A dynamic analysis of coupled hydrologic and chemical processes that determine solute transport. Water Resour. Res. 20, 1804–14.

Boano, F., Demaria, A., Revelli, R., Ridolfi, L., 2010. Biogeochemical zonation due to intrameander hyporheic flow. Water Resour. Res., 46, W02511, doi:10.1029/2008WR007583.

Bouwer, E.J., 1994. Bioremediation of chlorinated solvents using alternate electron acceptors. In: Norris, R.D., R.E. Hinchee, R. Brown, P.L. McCarty, L. Semprini, J.T. Wilson, D.H. Kampbell, M. Reinhard, E.J. Bouwer, R.C. Borden, T.M. Vogel, J.M. Thomas, and C.H. Ward, eds. Handbook of bioremediation. Boca Raton, FL: Lewis Publishers.

Bradley, P.M., 2003. History and ecology of chloroethene biodegradation: A review. Bioremediat. J., (7)81–109.

Bradley, P.M., 2011. Reinterpreting the importance of oxygen-based biodegradation in chloroethene contaminated groundwater. Ground Water Monit. R. 31(4), 50–55.

Bradley, P.M., Chapelle, F.H., 2011. Microbial mineralization of dichloroethene and vinyl chloride under hypoxic conditions. Ground Water Monit. R. 31(4), 39–49.

Canfield, D.E., 2001. Biogeochemistry of sulfur isotopes, in Valley, J.W. and Cole, D.R., eds., Reviews in mineralogy and geochemistry: Stable isotope geochemistry: Washington, D.C., Mineralogical Society of America, p. 607–636.

Cardenas, M.B., Cook, P.L.M., Jiang, H.S., Traykovski, P., 2008. Constraining denitrification in permeable wave-influenced marine sediment using linked hydrodynamic and biogeochemical modeling. Earth Planet Sci Lett. 275, 127–37.

Chapelle, F.H., 1996. Identifying redox conditions that favor the natural attenuation of chlorinated ethenes in contaminated groundwater systems. In: Symposium on Natural Attenuation of Chlorinated Organics in Ground Water, 17- 20, EPA/540/R-96/509.

Chapman, S.W., Parker, B.L., 2005. Plume persistence due to aquitard back diffusion following dense nonaqueous phase liquid removal or isolation. Water Resour. Res. 41 (12), W12411.

Chartrand, M.M., Waller, A., Mattes, T.E., Elsner, M., Lacrampe-Couloume, G., Gossett, J.M., Sherwood Lollar, B., 2005. Carbon isotopic fractionation during aerobic vinyl chloride degradation. Environ. Sci. Technol. 39(4), 1064–1070.

Cherry, J.A., Parker, B.L., 2006. Contaminant Transport Through Aquitards: A "State of the Science" Review. 147, Published by the Awwa Research Foundation.

Cohen, R.M. and Mercer, J.W., 1993. DNAPL Site Evaluation. C.K. Smoley/CRC Press, Boca Raton, Florida.

Davidson, E.A., Chorover, J., Dail, D.B., 2003. A mechanism of abiotic immobilization of nitrate in forest ecosystems: the ferrous wheel hypothesis. Global Change Biol. 9, 228-236.

Dincutoiu, I., Górecki, T., Parker, B.L., 2003. A novel technique for rapid extraction of volatile organohalogen compounds from low permeability media. Environ. Sci. Technol. 37(17), 3978–3984.

Dogramaci, S.S., Herczeg, A.L., Schiff, S.L., Bone, Y., 2001. Controls on $\delta^{34}S$ and $\delta^{18}O$ of dissolved SO_4 in aquifers of the Murray Basin, Australia and their use as indicators of flow processes. Appl. Geochem. 16, 475–488.

Engdahl, N.B., Vogler, E.T.,Weissmann, G.S., 2010. Evaluation of aquifer heterogeneity effects on river flow loss using a transition probability framework. Water Resour. Res. 46, W01506, doi:10.1029/2009WR007903.

Fleckenstein, J.H., Niswonger, R.G., Fogg, G.E., 2006. River-aquifer interactions, geologic heterogeneity, and low-flow management. Ground Water. 44, 837–52.

Flynn, S.J., Loffler, F.E., Tiedje, J.M., 2000. Microbial community changes associated with a shift from reductive dechlorination of PCE to reductive dechlorination of cis-DCE and VC. Environ. Sci. Technol. 34, 1056–1061.

Fowler, T., Reinauer, K., 2013. Enhancing Reductive Dechlorination With Nutrient Addition. Remed. J. 23 (1), 23–35.

Fukada, T., Hiscock, K.M., Dennis, P.F., Grischek, T., 2003. A dual isotope approach to identify denitrification in groundwater at a river bank infiltration site. Water Res. 37, 3070–3078.

Guilbeault, M.A., Parker, B.L., Cherry, J.A., 2005. Mass and flux distributions from DNAPL zones in sandy aquifers.Groundwater. 43(1), 70–86.

Gibson, B.D., Amos, R.T., Blowes, D.W., 2011. $^{34}S/^{32}S$ Fractionation during Sulfate Reduction in Groundwater Treatment Systems: Reactive Transport Modeling. Environ. Sci. Technol. 45, 2863–2870.

Goldscheider, N., Hunkeler, D., Rossi, P., 2006. Review: microbial biocenoses in pristine aquifers and an assessment of investigative methods. Hydrogeol. J. 14, 926–941.

Gossett, J.M., 2010. Sustained Aerobic Oxidation of Vinyl Chloride at Low Oxygen Concentrations. Environ. Sci. Technol. 44(4), 1405–1411.

Hartog, H., Cho, J., Parker, B.L., Annable, M.D., 2010. Characterization of a heterogeneous DNAPL source zone in the Borden aquifer using partitioning and interfacial tracers: Residual morphologies and background sorption. J. Contam. Hydrol. 115, 79–89.

Hill, A.R. 1990. Ground-water flow paths in relation to nitrogen chemistry in the nearstream zone. Hydrobiologia. 206, 39–52.

Holliger, C., Schumacher, W., 1994. Reductive dehalogenation as a respiratory process. Antonie Van Leeuwenhoek International Journal of General and Molecular Microbiology. 66(1–3), 239–246.

Hunkeler, D., Aravena, R., Berry-Spark, K., Cox, E., 2005. Assessment of degradation pathways in an aquifer with mixed chlorinated hydrocarbon contamination using stable isotope analysis. Environ. Sci. Technol. 39, 5975–5981.

Hwang, Y.K., Endres, A.L., Piggott, S.D., Parker, B. L., 2008. Long-term ground penetrating radar monitoring of a small volume DNAPL release in a natural groundwater flow field. J. Contam. Hydrol. 97(1), 1–12.

Jancin, M., Ebaugh, W.F., 2002. Shallow lateral DNAPL migration within slightly dipping limestone, southwestern Kentucky. Eng. Geol. 6(2–3), 141–149.

Johnston, D., 2006. Draft EPA Guidelines Regulatory monitoring and testing Groundwater sampling, 56, Environment Protection authority (EPA) Australia.

Kendall, C., 1998. Tracing nitrogen sources and cycling in catchments. In: Kendall, C. McDonnell, J.J. (Eds) Isotope Tracers in Catchment Hydrology, 521–576, Elsevier, Amsterdam.

Kouznetsova, I., Mao, X.M., Robinson, C., Barry, D.A., Gerhard, J.I., McCarty, P.L., 2010. Biological reduction of chlorinated solvents: Batch-scale geochemical modeling. Adv. Water Resour. 33, 969–986.

Lam, P., Kuypers, M.M.M., 2010. Microbial Nitrogen Cycling Processes in Oxygen Minimum Zones. Annu. Rev. Mar. Sci. 3, 317-45.

Lin, C., Larsen, E.I., Larsen, G.R., Cox, M.E., Smith, J.J., 2012. Bacterially mediated iron cycling and associated biogeochemical processes in a subtropical shallow coastal aquifer: implications for groundwater quality. Hydrobiologia. 696, 63–76.

Löffler, F.E., Tiedje, J.M., Sanford, R.A., 1999. Fraction of electrons consumed in electron acceptor reduction and hydrogen thresholds as indicators of halorespiratory physiology. Appl. Environ. Microb. 65, 4049–4056.

Luciano, A., Petrangeli Papini, M., Viotti, P., 2010. Laboratory investigation of DNAPL migration in porous media. J. Hazard. Mater. 176, 1006–1017.

Mariotti, A., Germon, J.C., Hubert, P., Kaiser, P., Letolle, R., Tardieux, A., Tardieux, P., 1981. Experimental determination of nitrogen kinetic isotope fractionation: some

principles; illustration for the denitrification and nitrification processes. Plant and soil, 62(3), 413–430.

Mason, B.J., 1992. Preparation of Soil Sampling Protocols: Sampling Techniques and Strategies EPA. 169.

Mayer, B., 2005. Assessing sources and transformations of sulfate and nitrate in the hydrosphere using isotopic techniques. In: Isotopes in the Water Cycle: Past, Present and Future of a Developing Sciences, Aggarwal, P.K., Gat J.R. & Froehlich, F.O. (ed), IEA, Netherlands.

Maymo-Gatell, X., Nijenhuis, I., Zinder, S.H., 2001. Reductive dechlorination of cis-1, 2-dichloroethene and vinyl chloride by "*Dehalococcoides ethenogenes*". Environ. Sci. Technol. 35 (3), 516–521.

McCarty, P.L., Smith. D.P., 1986. Anaerobic waste-water treatment 4. Environ. Sci. Technol. (20)12, 1200–1206.

Mercer, J.W., Cohen, R.M., 1990. Review of immiscible fluids in the subsurface. Properties models characterization and remediation. J. Contam. Hydrol. 6 (2), 107–163.

Palau, J., Soler, A., Teixidor, P., Aravena, R., 2007. Compound-specific carbon isotope analysis of volatile organic compounds in water using solid-phase microextraction. Journal of Chromatography 1163, 260–268.

Pankow F., Cherry J.A., 1996. Dense Chlorinated Solvents and Other DNAPLs in Groundwater: History, Behavior and Remediation. Waterloo press, Waterloo.

Pantazidou, M., Panagiotaki, I., Mamais, D., Zikidi, V., 2012. Chloroethene Biotransformation in the Presence of Different Sulfate Concentrations. Ground Water Monit. R. 32, 106–119.

Parker, B.L., Cherry, J.A., Chapman, S.W., 2004. Field study of TCE diffusion profiles below DNAPL to assess aquitard integrity. J. Contam. Hydrol. 74 (1-4), 197–230.

Parker, B.L., Cherry, J.A., Chapman, S.W., Guilbeault, M.A., 2003. Review and analysis of chlorinated solvent DNAPL distributions in five sandy aquifers. VZJ. 2 (2), 116–137.

Puigserver, D., 2010. Field and laboratory techniques for characterizing soil and groundwater DNAPL contamination episodes for establishing remediation strategies (Tècniques de camp i laboratori per a la caracterització d'episodis de contaminació per DNAPL en sòls i aigües subterrànies per a l'establiment d'estratègies de remediació), 919, Doctoral Thesis University of Barcelona, Barcelona-Spain.

Puigserver, D., Carmona, J.M., Cortes, A., Viladevall M., Arce, M., Barker J., Vandergriendt, M., 2008. Application of a Characterization Methodology of DNAPL Contaminant Episodes Based on the Integration of Field and Laboratory Tools. Proceedings of the Sixth International Conference on Remediation of Chlorinated and Recalcitrant Compounds (Monterey, CA; May 2008). Battelle Press, Columbus, OH, ISBN 1-57477-163-9, Paper F-010, 8 pp.

Puigserver, D., Carmona, J.M., Cortés, A., Viladevall, M., Nieto, J.M., Grifoll, M, Vila, J., Parker, B.L., 2013. Subsoil heterogeneities controlling porewater contaminant mass and microbial diversity at a site with a complex pollution history. J Contam Hydrol. 144 (1), 1–19.

Puls, R.W., Barcelona, M.J., 1996. Low-flow (minimal drawdown) ground-water sampling procedures, 12, Ground Water Issue, EPA.

Rivett, M.O., 1995. Soil-gas signatures from volatile chlorinated solvents: Borden field experiments. Ground Water. 33, 84–98.

Robson, S.G., 1993. Techniques for estimating specific yield and specific retention from grain-size data and geophysical logs from clastic bedrock aquifers. US Department of the Interior, US Geological Survey.

Scheutz, C., Broholm, M.M., Durant, N.D., Weeth, E.B., Jørgensen, T.H., Dennis, P., Jacobsen, C.S., Cox, E.E., Chambon, J.C., Bjerg, P.L., 2010. Field evaluation of biological enhanced reductivedechlorination of chloroethenes in clayey till. Environ. Sci. Technol. 44 (13), 5134–5141.

Schwientek, M., Einsiedl, F., Stichler, W., Stögbauer, A., Strauss, H., Maloszewski, P., 2008. Evidence for denitrification regulated by pyrite oxidation in a heterogeneous porous groundwater system. Chem. Geol. 255 (1–2), 60–67.

Silva, S.R., Kendall, C., Wilkinson, D.H., Ziegler, A.C., Chang, C.C.Y., Avanzino, R.J., 2000. A new method for collection of nitrate from fresh water and the analysis of nitrogen and oxygen isotope ratios. J. Hydrol. 228, 22–36.

Smith, J.W.N., Surridge, B.W., Haxton, T.H., Lerner, D.N., 2009. Pollutant attenuation at the groundwater–surface water interface: A classification scheme and statistical analysis using national-scale nitrate data. J. Hydrol. 369(3), 392-402.

Steinbach, A., Seifert, R., Annweiler, E., Michaelis, W., 2004. Hydrogen and carbon isotope fractionation during anaerobic biodegradation of aromatic hydrocarbons a field study. Environ. Sci. Technol, 38(2), 609–616.

Stuyfzand, P.J., Juhàsz-Holterman, M.H.A., de Lange, W.J., 2006. Riverbank filtration in the Netherlands: well fields, clogging and geochemical reactions. Riverbank Filtration Hydrology. Springer Netherlands. 119–153.

Tiehm, A., Schmidt, K.R., 2011. Sequential anaerobic/aerobic biodegradation of chloroethenes—aspects of field application. Curr. Opin. Biotech. 22, 415–421.

Tobiszewski, M., Namieśnik, J., 2012. Abiotic degradation of chlorinated ethanes and ethenes in water. Environ. Sci. Pollut. Res. Int. 19(6),1994–2006.

USEPA (2008) A guide for assessing biodegradation and source identification of organic ground water contaminants using compound specific isotope analysis (CSIA). Office of Research and Development, Ada, Oklahoma

Van der Zaan, B., Hannes, F., Hoekstra, N., Rijnaarts, H., de Vos, W.M., Smidt, H., Gerritse, J., 2010. Correlation of Dehalococcoides 16S rRNA and chloroethene-reductive dehalogenase genes with geochemical conditions in chloroethene-contaminated groundwater. Appl. Environ. Microbiol., 76, 843–850.

Vitoria, L., Otero, N., Soler, A., Canals, A., 2004. Fertilizer characterisation: isotopic data (N, S, O, C and Sr). Environ. Sci. Technol. 38, 3254–3262.

Vogel, T.M., Criddle, C.S., McCarty, P.L., 1987. Transformations of Halogenated Aliphatic Compounds. Environ. Sci. Technol. 21 (8), 722–736.

Vogel, T.M., McCarty, P.L., 1985. Biotransformation of tetrachloroethylene to trichloroethylene, dichloroethylene, vinyl chloride, and carbon dioxide under methanogenic conditions. Appl. Environ. Microbiol. 49(5):1080–1083.

Wei, N., Finneran, K.T., 2011. Influence of ferric iron on complete dechlorination of trichloroethylene (TCE) to ethene: Fe(III) reduction does not always inhibit complete dechlorination. Environ. Sci. Technol. 45 (17), 7422–7430.

Wexler, S.K., Hiscock, K.M., Dennis, P.F., 2012. Microbial and hydrological influences on nitrate isotopic composition in an agricultural lowland catchment. J. Hydrol. 468, 85–93.

Wiedemeier, T.H., Wilson, J.T., Hansen, J.E., Chapelle, F.H., Swanson, M.A., 1996. Technical Protocol for Evaluating Natural Attenuation of Chlorinated Solvents in Groundwater. Revision 1. AIR FORCE CENTER FOR ENVIRONMENTAL EXCELLENCE BROOKS AFB TX.

Yang, Y., McCarty, P.L., 1998. Competition for hydrogen within a chlorinated solvent dehalogenating anaerobic mixed culture. Environ. Sci. Technol. 32 (14), 3591–3597.

Zhang, Y.C., Slomp, C.P., Broers, H.P., Bostick, B., Passier, H.F., Böttcher M.E., Omoregie, E.O., Lloyd, J.R., Polya, D.A., Cappellen, P.V., 2012. Isotopic and

microbiological signatures of pyrite-driven denitrification in a sandy aquifer. Chem Geol. 300-301, 123–132.

FIGURE CAPTIONS

Figure 1. A) Location map of the three source areas. Geological map and water table map in November 2009 (potentiometric lines in m.a.s.l.). In the source areas B and C, the riverbed of River Ges is formed by the Quaternary gravel paleochannels and silty materials that connect both banks of the river. B) Close-up map of the source area C (study zone) showing the location of profiles A-A', B-B' and C-C'.

Figure 2. Annual average values of temperature and EC in profiles A-A' (source zone) and C-C' (along flow) and in the River Ges. Location of the profiles in Figure 1.

Figure 3. Annual average values of TOC and DO in profiles A-A' (source zone), B-B' and C-C' (along flow) and in the River Ges. Location of the profiles in Figure 1.

Figure 4. A) Nitrate variation along groundwater flow. B) Isotopic composition of nitrate in source area C (November 2009). More negative values in $\delta^{15}N_{nitrate}$ and $\delta^{18}O_{nitrate}$ indicate lower isotopic fractionation (i.e., a less advanced biodegradation process, and vice versa). Yellow dots: piezometers from profile A-A' (source zone). Bottom plot corresponds to Kendall (1998).

Figure 5. A) Sulfate variation along groundwater flow. B) Isotopic composition of sulfate in source area C (November 2009). More negative values in $\delta^{34}S_{sulfate}$ and $\delta^{18}O_{sulfate}$ indicate lower isotopic fractionation (i.e., a less advanced biodegradation process, and vice versa). Yellow dots: piezometers from profile A-A' (source zone). Bottom plot corresponds to Vitoria et al. (2004). The sulfide oxidation box is from Mayer (2005).

Figure 6. Profile A-A' (parallel to River Ges). SD29, S3 and SD32 are located in gravel paleochannels. SD28, S1, SD30 and SD31 are located in fine sands and silts. Location of profile in Figure 1. A) Total molar concentrations and molar fractions of dissolved chloroethenes. DO values at piezometers during the sampling surveys are shown below each circular plot (mg/L). B) Isotopic composition of chloroethenes (dashed line: $\delta^{13}C_{PCE}$ of spilled DNAPL obtained from piezometer S2). More negative values in $\delta^{13}C_{PCE}$ indicate lower isotopic fractionation (i.e., a less advanced biodegradation process, and vice versa).

Figure 7. Profile B-B' (along groundwater flow). Location of profile in Figure 1. A) Total molar concentrations and molar fractions of dissolved chloroethenes. DO values at piezometers during the sampling surveys are shown below each circular plot (mg/L). B) Isotopic composition of chloroethenes (dashed line: $\delta^{13}C_{PCE}$ of spilled DNAPL obtained from piezometer S2). More negative values in $\delta^{13}C_{PCE}$ indicate lower isotopic fractionation (i.e., a less advanced biodegradation process, and vice versa).

Figure 8. Profile C-C' (along groundwater flow). Location of profile in Figure 1. A) Total molar concentrations and molar fractions of dissolved chloroethenes. DO values at piezometers during the sampling surveys are shown below each circular plot (mg/L). B) Isotopic composition of chloroethenes (dashed line: $\delta^{13}C_{PCE}$ of spilled DNAPL obtained from piezometer S2). More negative values in $\delta^{13}C_{PCE}$ indicate lower isotopic fractionation (i.e., a less advanced biodegradation process, and vice versa).

Figure 9. A) Distribution of $\delta‰^{34}S_{sulfate}$ and $\delta‰^{15}N_{nitrate}$ along flow in the studied profiles. B) $\delta^{13}C_{PCE}$ vs $\delta^{15}N_{nitrate}$ in the source and along flow. C) $\delta^{13}C_{PCE}$ vs $\delta^{34}S_{sulfate}$ in the source and along flow. In these plots, more negative values in δ values indicate lower isotopic fractionation (i.e., a less advanced biodegradation process, and vice versa).

TABLE CAPTION

Table 1. Depths at which residual DNAPL was detected in piezometers when drilling the boreholes.

Table 1

Click here to download Table: Table 1 (V2).docx

Piezometer	Depth (m)	Location	Depths of screened zone in the alluvial aquifer	
			upper part (m)	lower part (m)
S5	1.8	On a silt level interbedded between gravels (in the water table fluctuation zone)	1.5	3.0
	3.4	On the contact with marlstones of bedrock (below the minimum water table)		
S2	2.75	On a silt level interbedded between gravels (in the water table fluctuation zone)	2.0	3.0
	3.3	On a silt level interbedded between gravels (below the minimum water table)		
	3.4	On the contact with the marlstones of the bedrock (below the minimum water table)		
SD29	4.5	On a silt level interbedded between gravels, near the contact with the marlstones of the bedrock (below the minimum water table)	2.1	5.1
SD28	1.8	On a silty clay level interbedded between gravels, near the contact with the marlstones of the bedrock (below the minimum water table)	1.0	2.1
SD58	4.5	On a silty clay level interbedded between gravels, near the contact with the marlstones of the bedrock (below the minimum water table)	4.0	4.8
SD18	4.7	On the contact with the marlstones of the bedrock (below the minimum water table)	2.4	4.7

Figure 1

Click here to download high resolution image

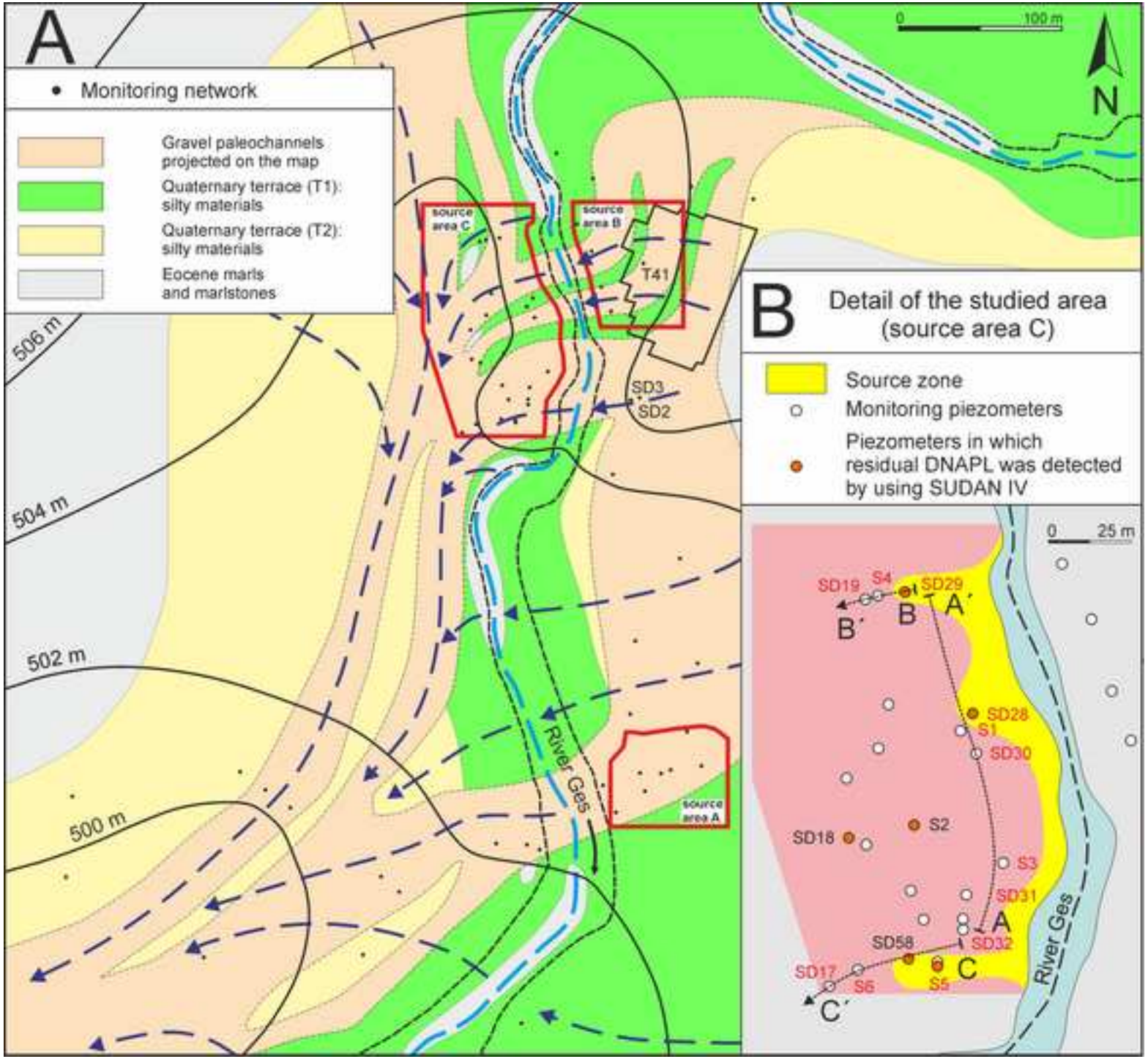

Figure 2

Click here to download high resolution image

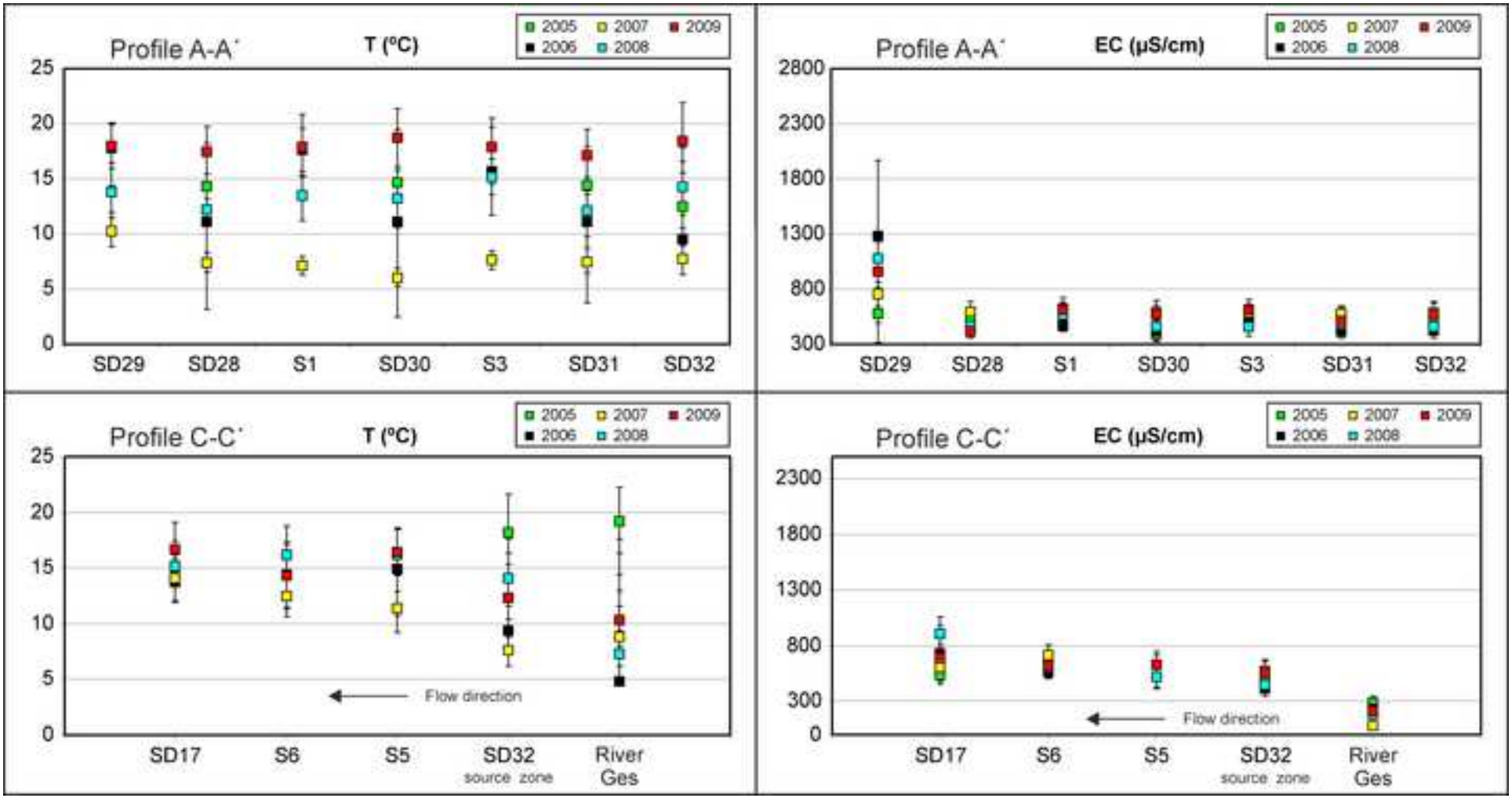

Figure 3

Click here to download high resolution image

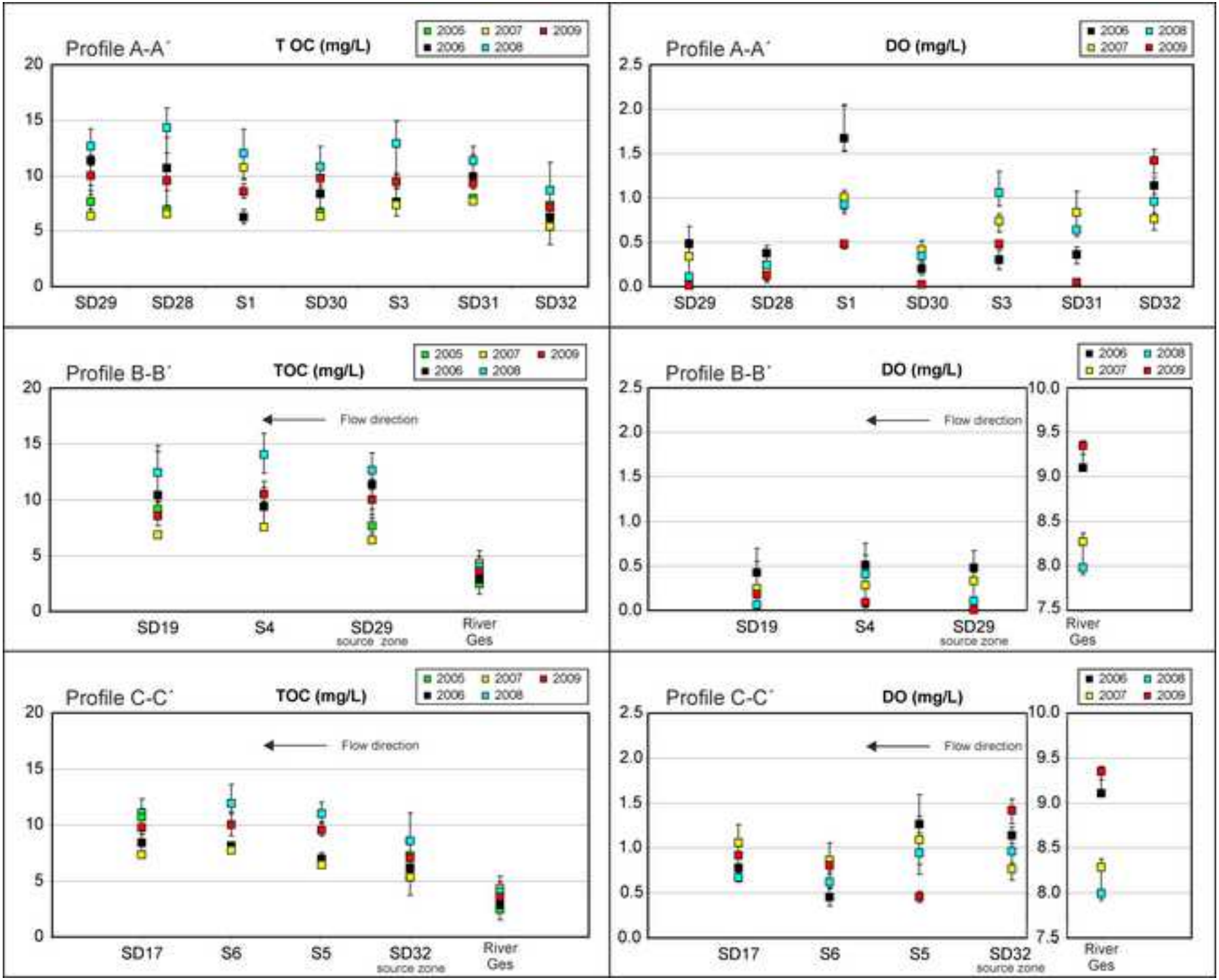

Figure 4

Click here to download high resolution image

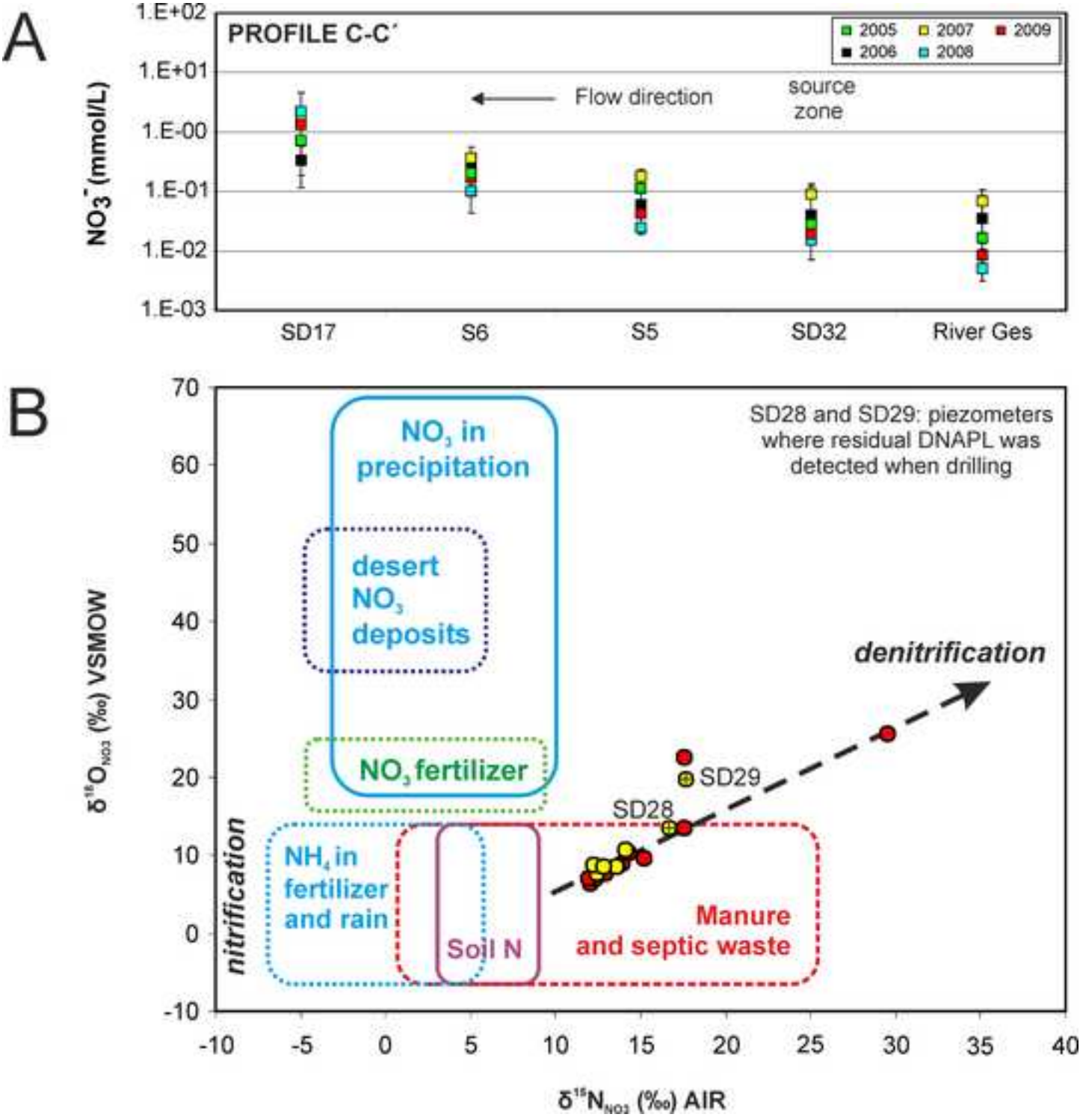

Figure 5

Click here to download high resolution image

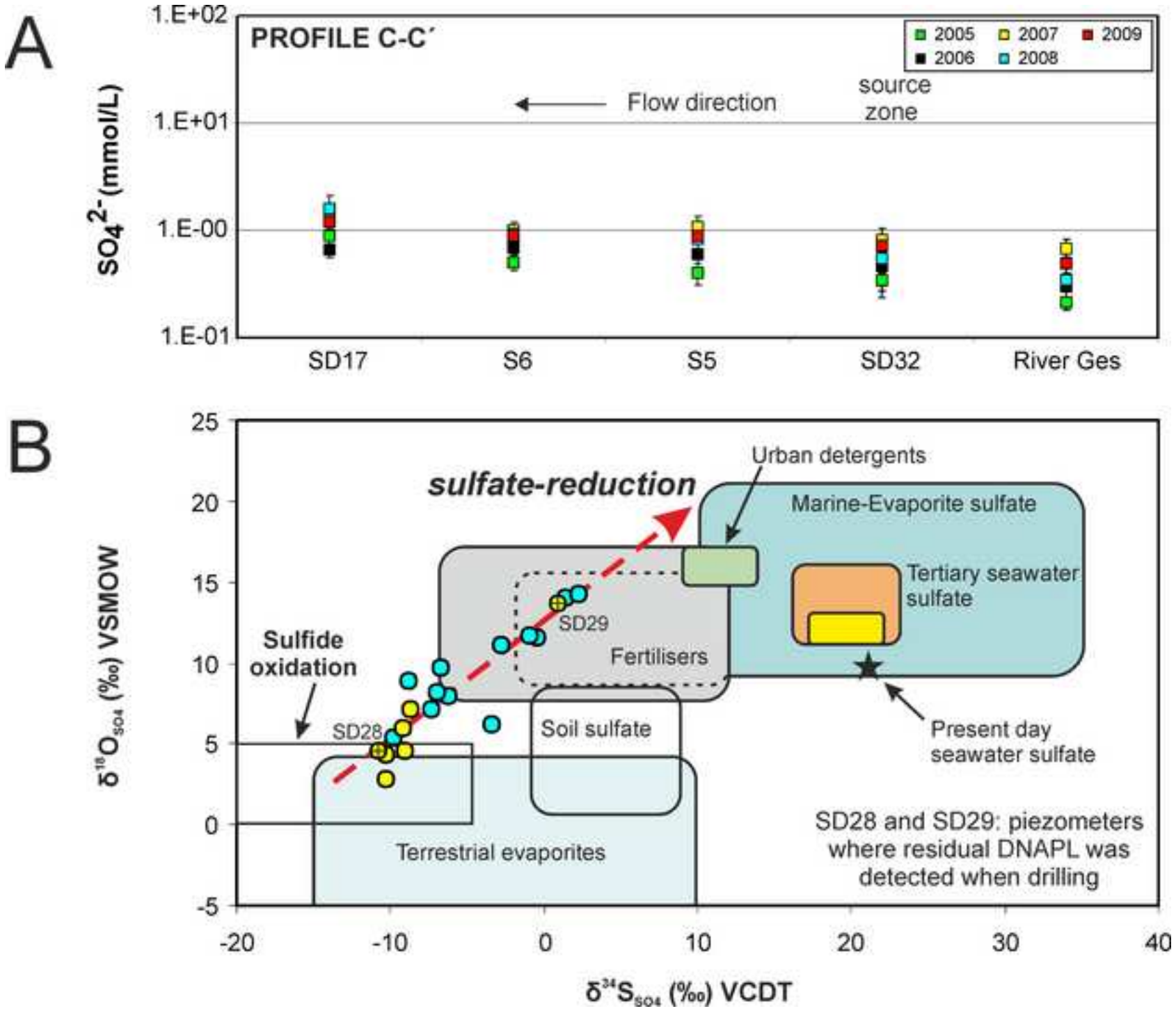

Figure 6

Click here to download high resolution image

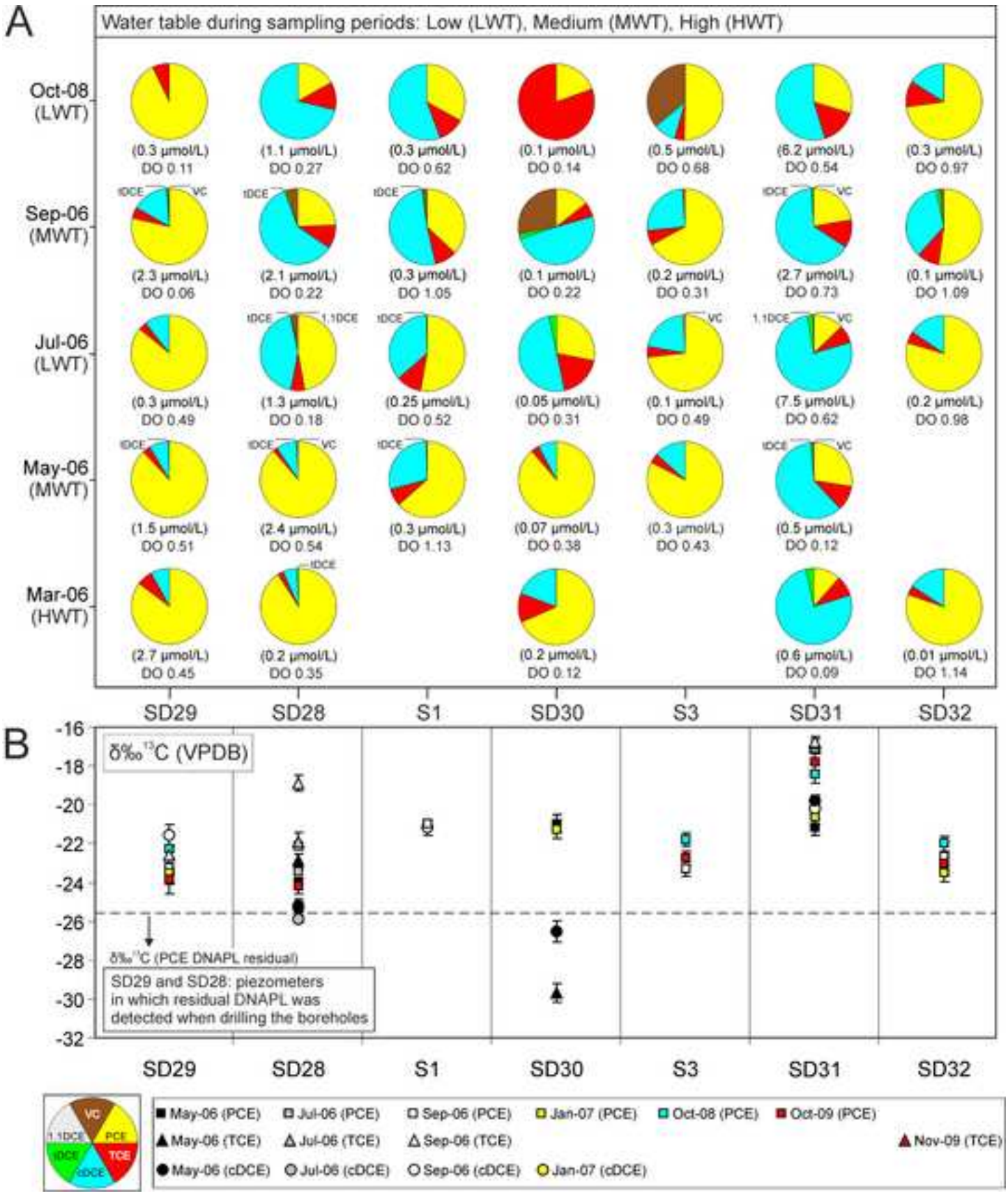

Figure 7

Click here to download high resolution image

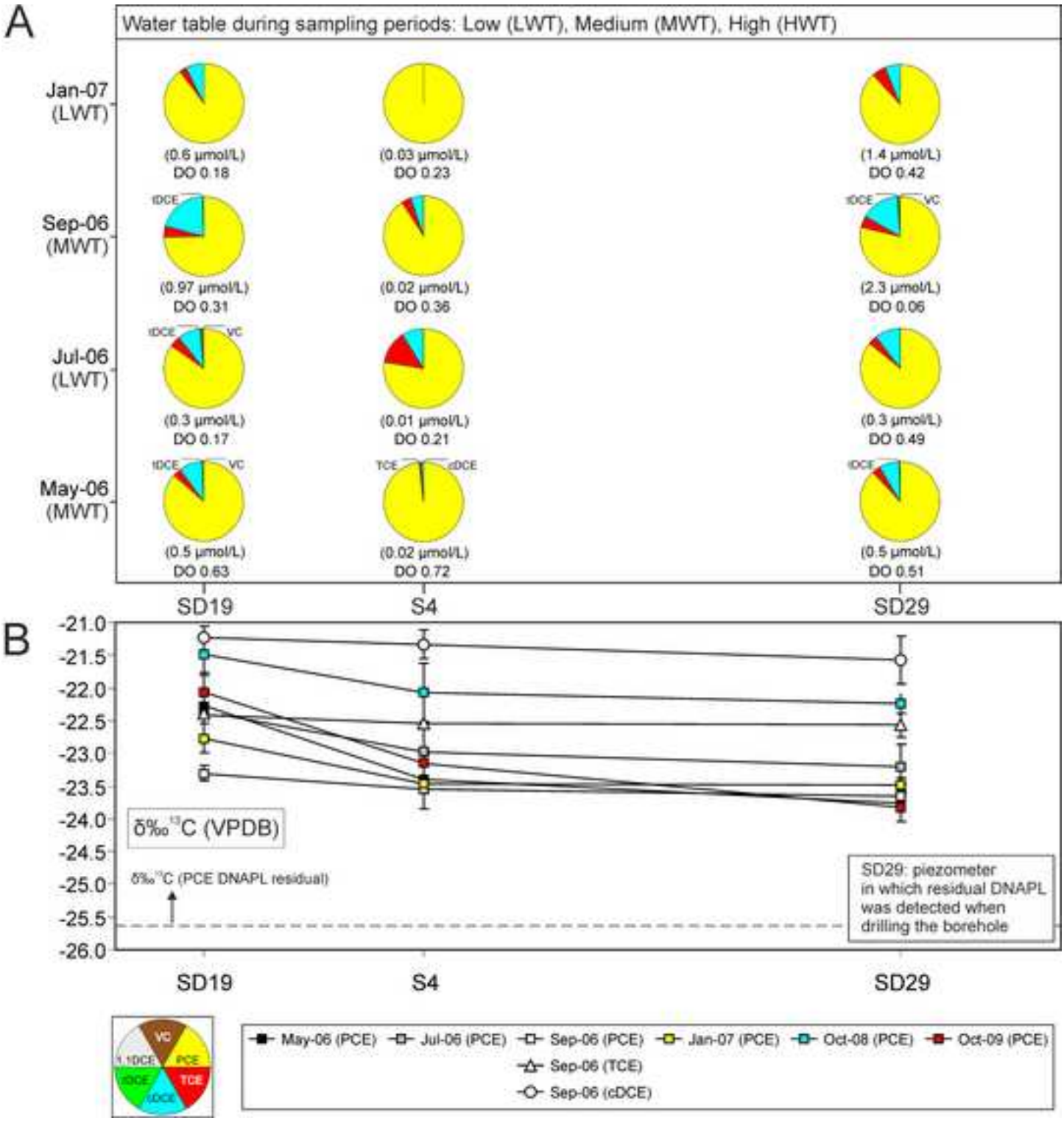

Figure 8

Click here to download high resolution image

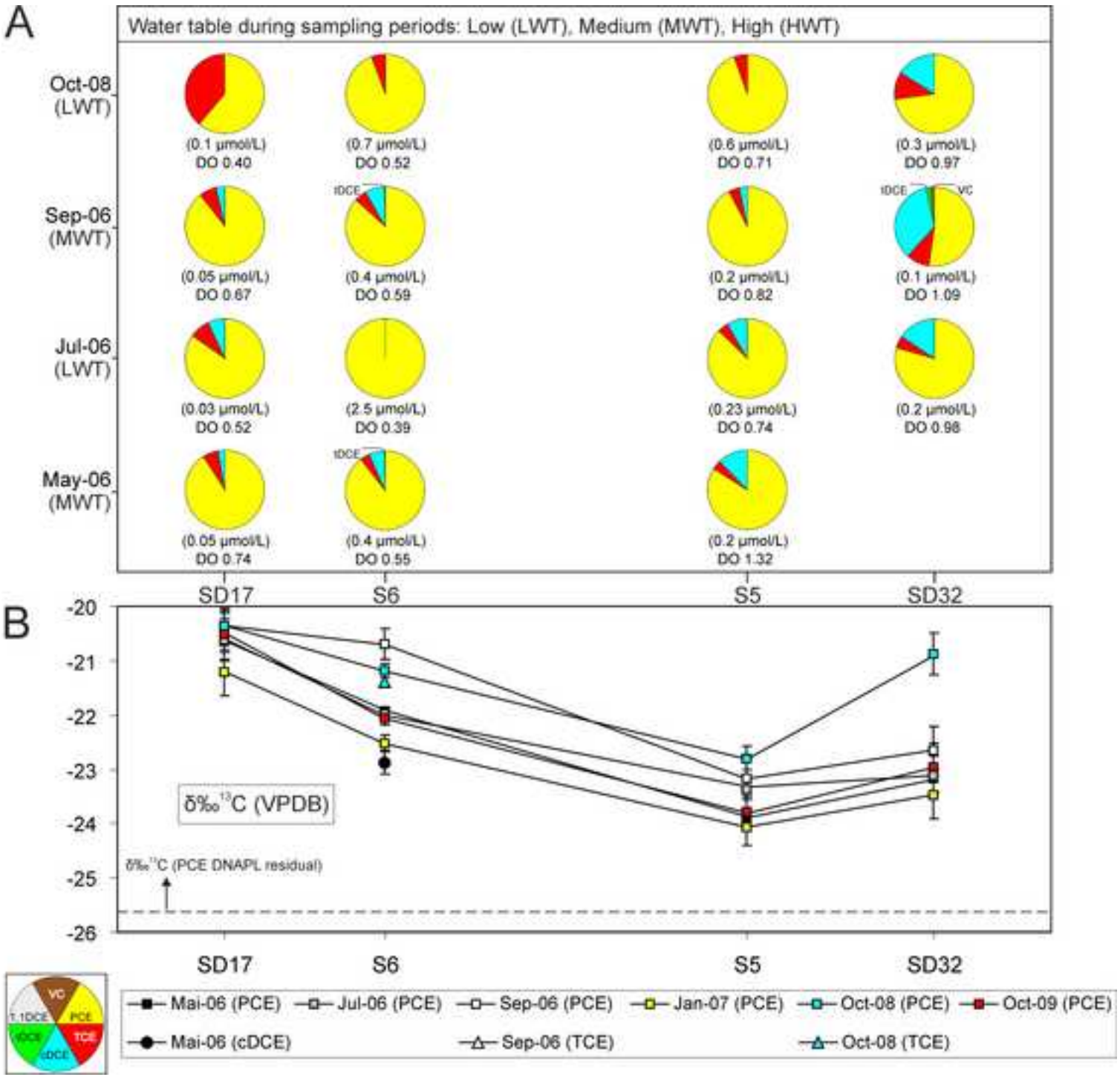

Figure 9

Click here to download high resolution image